

Mathematical Model to Predict Combustion Pressure in a Direct Injection Diesel Engine: Part-I

Ramendra Singh Niranjan, Department of Mechanical Engineering, UIET, CSJM University Kanpur, 208024, India

Bristi Mitra, Department of Chemical Engineering, UIET, CSJM University Kanpur, 208024, India

Rajesh Kumar Prasad, Department of Mechanical Engineering, ICFAI University Jharkhand, Ranchi-835222, India

*Corresponding Author:rajeshp2010@gmail.com

Abstract.

Diesel engine are most popular since last century because of higher power density and still used in transportation sector. This study is focused on the simulation and experimental investigation of simplified model for prediction of combustion pressure in a direct injection diesel engine. It was observed that predictions of pressure traces at different operating modes are very accurate from full load to 10% load with varying engine speed. The deviation of peak pressures at 100% load both at 2200 rpm & 1400 rpm are 9% and 3.4% respectively. It was also observed that as load on engine reduced than corresponding peak pressure reduces.

Keywords: Direct injection diesel engine, mathematical model, combustion pressure, zero dimensional two-zone combustion model

Introduction

Efficient diesel engines are the most popular in transportation sector due to higher power to weight ratio [1] but most polluting among all alternative liquid fuels result several environmental complications. To design and develop new engines, R&D cost and time needed for it can be reduced by developing simulation model. Engine design parameters are basic input to these model and rest other parameters predicted by these model for active control of diesel combustion and emissions [2, 3]. Oxides of nitrogen (NOx) and particulate matter (PM) are main pollutants in diesel engines. NOx formation in either diesel or gasoline engine is mainly governed by temperature exponentially but it reduced by leaning the mixture [4] In this study, only combustion prediction model was considered [5-8] which having direct relation with temperature [9]. There are two categories of models used to describe diesel combustion, comprehensive three-dimensional models and phenomenological models or zero dimensional models. Three -dimensional models use computational fluid dynamic (CFD) codes to describe the flow field and temperature conditions in the combustion chamber. Sub models are included for spray breakup, ignition, heat transfer, and pollutant formation. Phenomenological models separate the combustion chamber into different zones and can be categorized by the number of these zones. There are one, two, three, and multi-zone models. These models are often called zero -dimensional because they provide no spatial resolution. More detailed explanations of these mode types can be found in [10] and [11].

Three-Dimensional Models: CFD has been used extensively for modelling engines. In addition to modelling the three-dimensional flow, engine CFD codes require a moving boundary condition for piston movement. With a complex flow model it is normally necessary to model combustion using the same type of correlations that are used in zero dimensional models. This diminishes the benefits of 3-D models. Due to the complexity of these models, they demand large amounts of computer power. The time required for the calculations is also limiting. This is especially important when much iteration are required to determine constants or to determine the effects of changing parameters

Single-Zone Models: Single zone models are advantageous because of their simplicity and are widely used along with empirical data within the engine industry to make design decisions. This method assumes that the entire volume of the combustion chamber is a homogeneous mixture of air and combustion products. It then assumes that the fuel is burned immediately on injection into the combustion chamber [11]. Examples of this type of model can be found in [10]. Often, the measured pressure rise in an engine is used to tune the model or is used to provide a rate of heat release. Zero dimensional models are therefore usually not entirely predictive but are used to extend the value of the measured data. The disadvantage of single zone models is that they cannot fully describe the complex phenomena that comprise the compression-ignition engine combustion process and substantial empirical input must be used [10].

Two-Zone Models: A two -zone model separates the combustion chamber into a fuel/air mixture zone (zone 1) and a zone of air and combustion products (zone 2). This two -zone structure is used extensively in spark ignition engine models [11].

Three-Zone Models: Foster [11] describes a model that uses three zones to describe combustion in an ethanol fumigated diesel engine. In this model two of the zones contain the air-fuel mixture. Zone 1 contains air and ethanol, and zone 2 contains diesel fuel, air, and ethanol. The third zone contains the products of combustion. The diesel fuel is assumed to burn first, resulting in the destruction of one of the air-fuel zones. The air-ethanol zone is then assumed to burn.

Multi-Zone Models: Multi-zone models separate the fuel spray into a large, finite number of zones. In one, the zones are small packets of fuel that move through the combustion chamber. The state of the mass in each packet is tracked as it moves.

Johansson et al, [12] developed NOx prediction model suitable for vehicle on-board, on-line implementation. This study focused on different method to handle temperature calculations within the different zones avoiding iterative energy balance computation. A two-zone model, one burned zone in which the NOx formation takes place and one unburned zone composed of only air. The burned zone temperature was computed using knowledge about the number of moles in the different zones and the global temperature as well as the temperature of the unburned zone (under the assumption of isentropic compression).

Mellor et al, [13] developed a skeletal mechanism consisting of seven elementary reactions is used to develop a two-zone model for NOx emissions from DI Diesel engines. Zone-1 is a near stoichiometric region ($\Phi=1$) where [NO] is small and in which NO formation occurs through forward reactions. Zone-2 is a region in which hot, burned gases are present at the overall equivalence ratio.

Experimental Setup and Methodology

The model used in this paper is zero-dimensional because it does not account for exact geometric features of the engine or combustion chamber. The cylinder content is considered as an ideal gas. Input required for predicting combustion pressure are engine bore, stroke, connecting rod length, Compression ratio, inlet and exhaust valve timing, Operating speed, Fuel injected quantity, start of injection, duration of injection, Inlet manifold pressure and temperature, Air intake depression and back pressure and fuel cetane number and lower calorific value.

In two- zone model, one burned zone in which the NOx formation takes place and one unburned zone composed of only air and EGR, as explained by Figure 1.

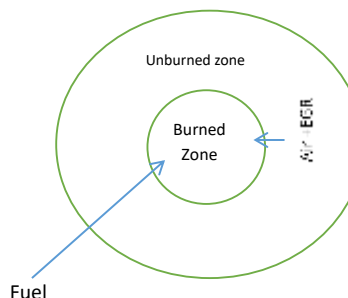
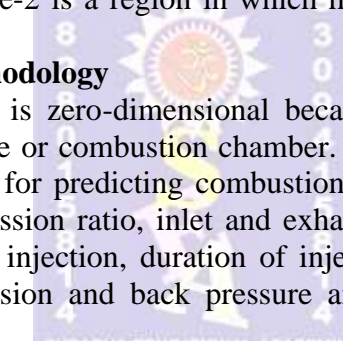


Figure 1: Two zone concept [6]

All the assumptions made in this model are listed below:

- Zero dimensional two zone model.
- The cylinder content can be described as an ideal gas.
- Unburned cylinder air is compressed and expanded isentropically.
- Combustion takes place at local stoichiometric conditions.
- There are no pressure gradients inside the cylinder.
- NO is formed in the burned zone.

- All injected fuel is fully burned.
- The ideal gas law is valid for each zone separately and for the compete combustion chamber.
- All released energy originates from injected fuel.
- Species in the burned zone are in equilibrium.
- There is no heat transfer among the zones.

In this work the burned zone temperature was calculated using knowledge about the mass in the different zones and using energy balance approach. Furthermore it is possible to compute the mass in the burned zone using ‘conventional’ heat release analysis [3]. It is also possible to compute the total mass in the combustion chamber and hence mass in the unburned zone.

Figure 2 shows experimental setup of turbocharged diesel engine which is coupled with eddy current dynamometer. The engine specification is provided in Table 1.

Table 1: Engine specification

Parameter	Specifications
Engine Model	4- cylinder Turbocharged DI Diesel
Bore (mm)/ Stroke (mm)	102/ 110
Connecting rod length (mm)	220
IVC (CA)/ EVO (CA)	210/ 540
Rated speed (rpm)	2200
Compression ratio/ Swept volume (liter)	17.4/ 0.9 per cylinder
Injection system	Common rail

The engine suction side is fitted with air-conditioning system, air measuring system, and fuel measuring unit while exhaust side is partially connected to emission analyzer. AVL Indiset, was used as data acquisition system.

Un-cooled pressure transducer (GM12D) was used to acquire the in-cylinder pressure data vs. crank angle. AVL 365C angle encoder was used to convert the analogue angle pulses into digital output signals and it determines the position of the shaft w.r.t. TDC. The parameters noted from the engine experiment were in-cylinder gas pressure measurement (bar), and Fuel consumption(kg/ hr) for this paper point of view.

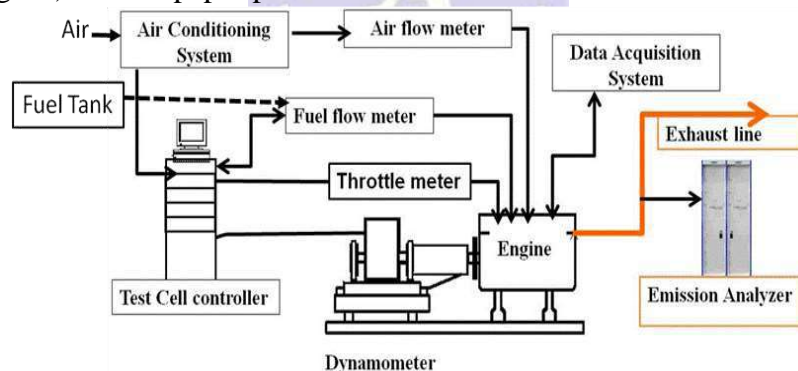


Fig.2. Engine experimental setup to collect data for validation of simulated results

Results and discussion

The first phase of experiments has been carried out on a 4-cylinder turbocharged DI Diesel engine. Diesel combustion was extensively studied by varying load at a speed of 2200 rpm and a BMEP of 8.6 bar by keeping constant injection timing. Intake manifold temperature was maintained at 105°C by providing cooling system, and compression ratio of 17.5. The engine tests were done according to standard IS: 10000. Parameters like the speed of the engine, fuel and air flow rate, power, exhaust gas temperature, inlet air temperature and oil temperature were recorded and data has been used to compute other parameters. During the experiments every measurement was recorded average data of 30s at the end of 5 min stabilization of engine for every change of conditions.

Effect of engine load on peak pressure

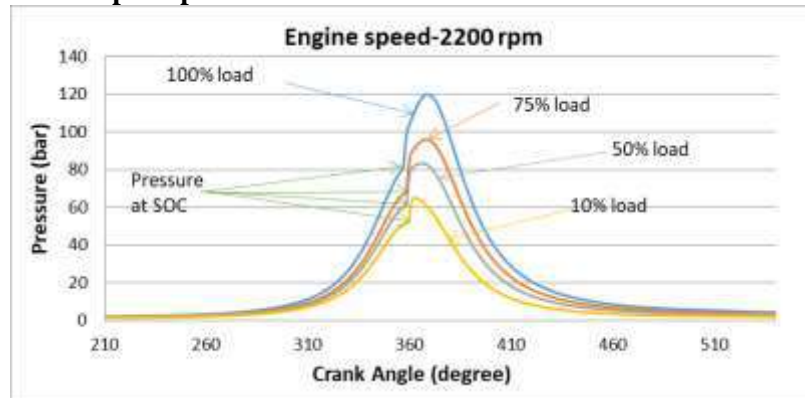


Figure 3: Comparison of Pressure traces at different loads

Figure 3 compare predicted and measured cylinder pressure traces at different loads at 2200 rpm. The maximum pressure at full load is 120 bar while at 10% load is 61.75 bar. It is observed that as load on engine decreases than corresponding peak pressure decreases. This is mainly due to two reasons: (i) as load on engine decreases than corresponding mass of fuel injected decreases, results lower heat release and peak pressure, and (ii) at lower load both inlet temperature and pressure are low which results lower pressure and temperature at Start of Combustion (SOC). Due to difference in inlet condition, the slopes of various pressure curves are deviates as shown in figure 3. As load decreases, exhaust gas temperature decreases with the leaner engine operation. With less energy to be recovered in comparison to high load in the turbocharger, the resulting boost pressure decreases. More in depth clarification is given in following paragraph.

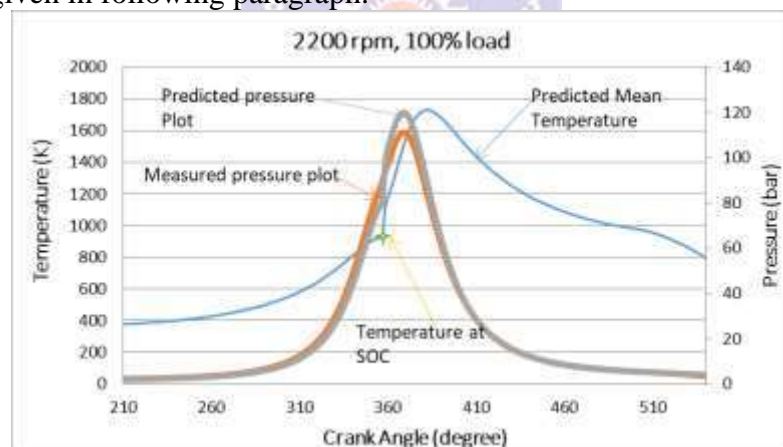


Figure 4: Comparison of Measured Vs. Predicted pressure plot at 2200 rpm and 100% load. In first operating mode (i.e. 2200 rpm and 100% load), both pressure and temperature at inlet to engine and start of combustion (SOC) are 2 bar, 80 bar and 378.3 K, 925.6 K respectively. Figure 4 shows the pressure and temperature at SOC after compression. The measured pressure at this mode was 110 bar at 363 degree CA which is very close to the predicted 364.4 degree CA. At this load, mass of air (387.5 Kg/hr) entrapped into the cylinder is also more which results higher pressure and temperature after compression.

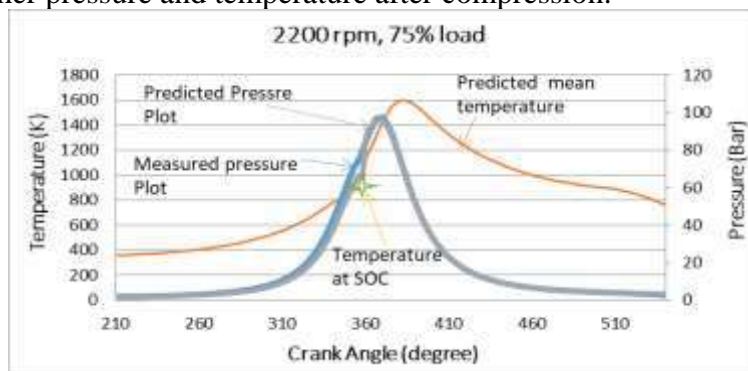


Figure 5: Comparison of Measured Vs. Predicted pressure plot at 2200 rpm and 75% load

In second operating mode ,the peak pressure observed at 75% load and 2200 rpm speed is 95 bar at 367 degree CA as shown in figure 5. The peak pressure during experiment was also 95 bar but at 365.5 degree CA . There is no difference in peak pressures and timing of occurrence of the peak pressures or pressure is precisely predicted by the model. It is also observed that due to decrease in load from 100% to 75%, pressure decrease from 120 bar to 95 bar but occurrences of peak pressures delayed by 2.5 degrees CA. Reasons for this drop are that air flow rate into the cylinder is 348.8 Kg/hr which is lower than earlier mode (387.5 Kg/hr) and also the inlet pressure is 1.65 bar instead of 2 bar. Maintaining the same compression ratio, we get pressure and temperature at SOC are 62 bar and 876.8 K. Comparing the above two mode, the drop in pressure is 18 bar while drop in temperature is 48.8 K.

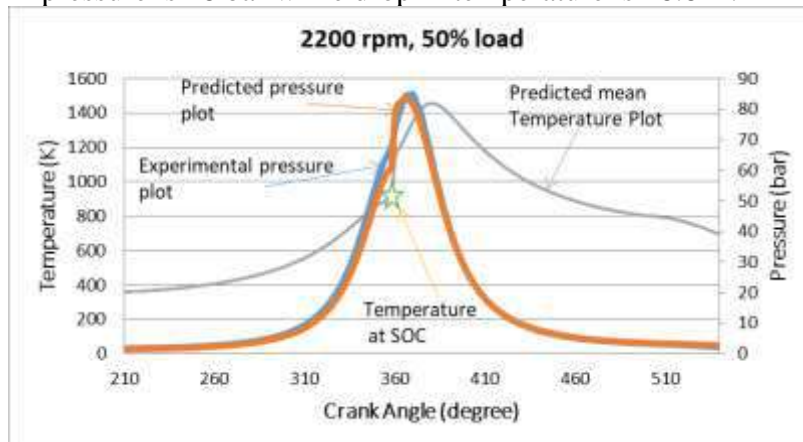


Figure 6: Comparison of Measured Vs. Predicted pressure plot at 2200 rpm and 50% load

In third operating mode, load on engine decreases from 75% to 50% at 2200 rpm then predicted peak pressure is also decreases from 95 bar to 83 bar as shown in figure 6. In this condition both the peak pressures i.e. predicted as well as measured are equal to 83 bar and their occurrences are 363.5 degree CA and 364 degree CA respectively. In this case, both air flow rate (309.8 Kg/hr) and inlet pressure are lower but equal inlet temperature results higher temperature at SOC (888.6 K due to low mass) and lower pressure(60.7 bar) than above two cases. This temperature is more than the pressure in second mode (876.8 K) because the inlet pressure is 1.48 bar which is lower than second mode (1.65 bar).

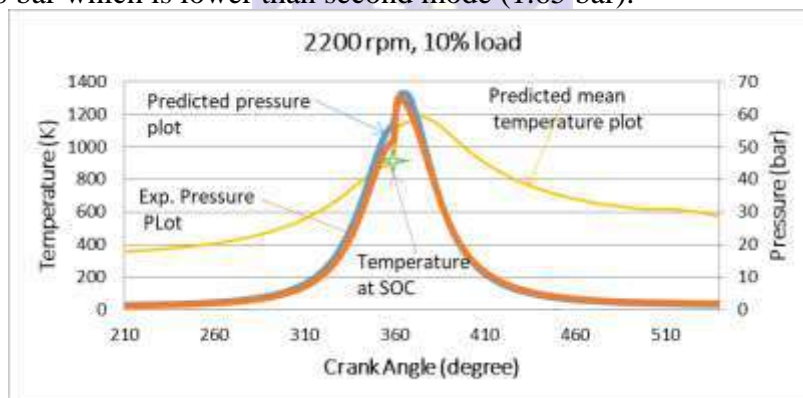


Figure 7: Comparison of Measured Vs. Predicted pressure plot 2200 rpm at 10% load

Again if load on engine further decrease from 50% to 10% at 2200 rpm (fourth operating mode) than in this mode also both predicted and measured pressures are same and equal to 65 bar. From figure 7, it is also observed that their occurrences are also same and equal to 362 degree CA. Inlet pressure is 1.25 bar while pressure at SOC is 51.6 bar. Due to same compression ratio but lower inlet pressure we get lower SOC pressure from earlier mode (60.7 bar) but temperature is nearly equal (888.7 K) because mass flow rate of air is (269.3 Kg/hr) low in this case and inlet temperatures are equal to 358.9K in both cases.

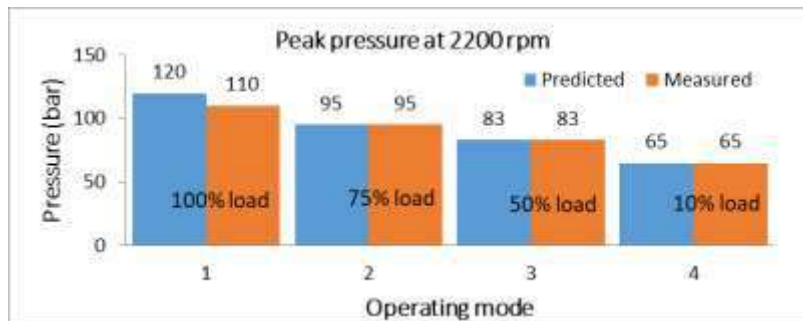


Figure 8: Peak pressures at different operating modes at 2200 rpm

The summary of the above four cases of peak pressures at 2200 rpm and different load conditions i.e. 100%, 75%, 50% and 10% are shown in figure 8.

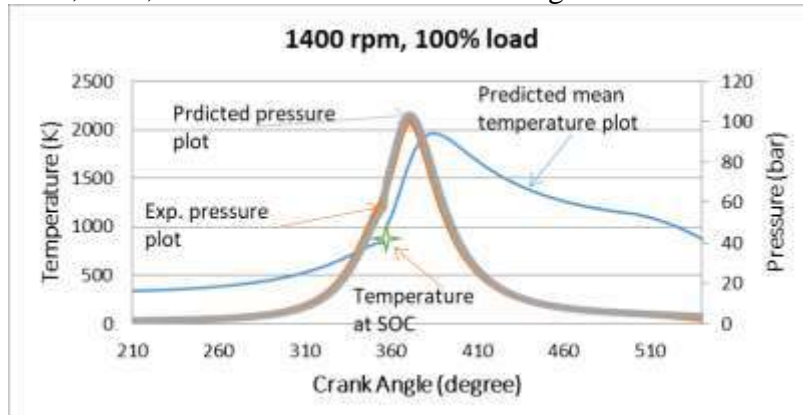


Figure 9: Comparison of Measured Vs. Predicted pressure plot at 1400 rpm at 100% load

In fifth case the engine was set at 1400 rpm at full load, the measured pressure was 100 bar which is slightly lower than predicted pressure of 103.4 bar. The full load pressure trace is shown in figure 9. The measured pressure occurred at 367.5 degree CA while predicted pressure is occurred at 370.5 degree CA. In comparison with 2200 rpm and full load, both fuel and air consumption per hour decreases (air required is 193.1 Kg/hr instead of 387.5 Kg/hr) but fuel consumption per cycle increase in 1500 rpm to overcome applied load. Both inlet and SOC conditions pressures and temperatures are 1.43 bar, 57.5 bar and 337.7 K, 837.7 K. Both pressure and temperature at SOC are low compared to first operating mode due to low input pressure and temperature in this mode.

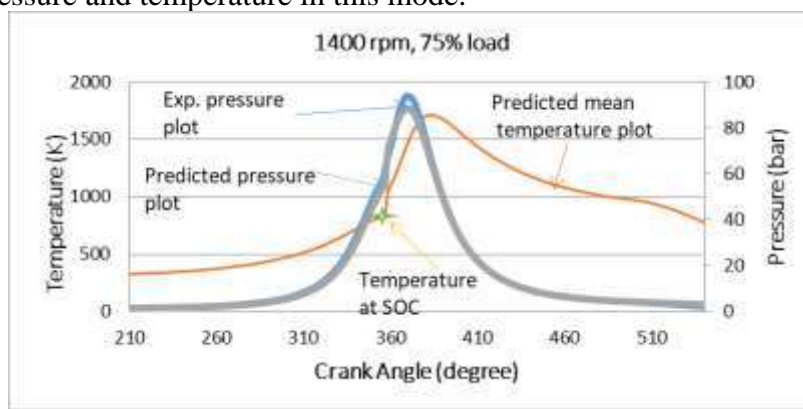


Figure 10: Comparison of Measured Vs. Predicted pressure plot at 1400 rpm and 75% load. If load on engine decreases from 100% to 75% at 1400 rpm then predicted peak pressure is also decreases from 103.4 bar to 88.4 bar as shown in figure 5.8. In this condition the peak pressures measured was equal to 91 bar and their occurrences are 369.5 degree CA and 367 degree CA respectively. The pressure and temperature at SOC are 54.3 bar and 801.4 K. Reasons for this drop are that air flow rate into the cylinder is 179.4 Kg/hr which is lower than earlier mode (193.1 Kg/hr) and also the inlet pressure is 1.32 bar instead of 1.43 bar. Comparing the above two mode, the drop in pressure is 3.2 bar while drop in temperature is 25.5 K.

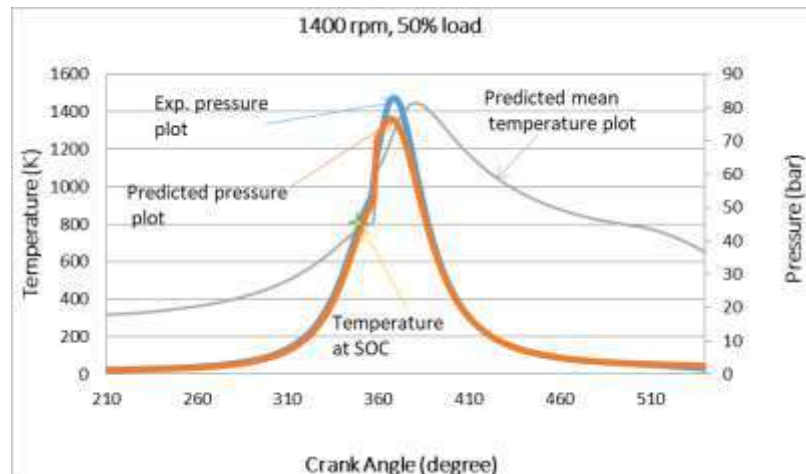


Figure 11: Comparison of Measured Vs. Predicted pressure plot 1400 rpm and 50% load
 Again if load on engine further decrease from 75% to 50% at 1400 rpm than in this also both predicted and measured pressures are equal to 76.6 bar and 81.5 bar respectively as shown in figure 11. It is also observed that their occurrences are equal to 366.5 degree CA and 366 degree CA. Both inlet and SOC conditions pressures and temperatures are 1.23 bar, 51.2 bar and 317.2 K, 801.4 K. Reason for this drop is due to low pressure and temperature at inlet compared to earlier mode.

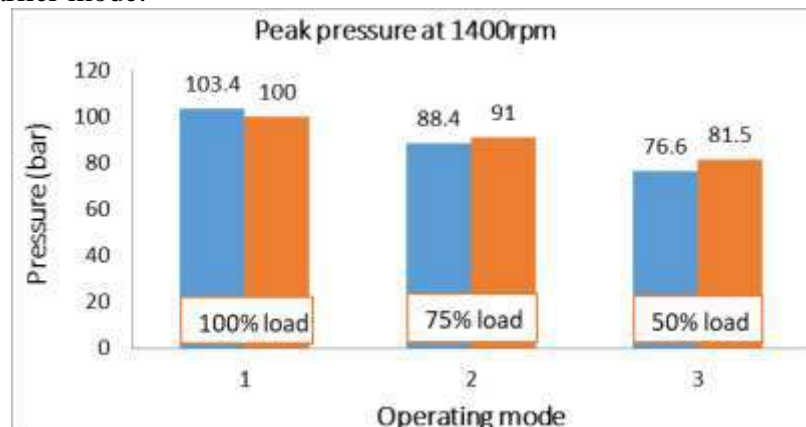


Figure 12: Peak pressure at different operating modes at 1400 rpm

Figure 12 shows that the comparison of measured vs. predicted peak pressures at three different load conditions i.e. 100%, 75% and 50% .

Conclusions

The combustion prediction model is developed with Precised accuracy for 4-stroke turbocharged DI diesel engine. In this work, different models were used for in-cylinder pressure predictions. The main findings of the work are summarised below:

- The predictions of pressure traces at different operating modes are very accurate from full load to 10% load. The deviation of peak pressures at 100% load both at 2200 rpm & 1400 rpm are 9% and 3.4% respectively. The deviations in peak pressures at Part loads i.e. 75%, 50%, and 10% load at 2200 rpm are nil. Similarly, deviation in peak pressures at 75% load and 50% at 1400 rpm are 2.8% and 6% respectively. . It is observed that as load on engine decreases than corresponding peak pressure decreases.
- Pressure and temperature at start of combustion mainly depend on inlet condition at inlet.
- Due to decrease in load on engine at particular rpm the rate of heat release decreases but when load is constant and engine speed decreases then rate of heat releases increases.

References

- [1] Agarwal, A.K., Shukla, P.C., Patel, C., Gupta, J.G., Sharma, N., Prasad, R.K. and Agarwal, R.A., 2016. Unregulated emissions and health risk potential from biodiesel

- (KB5, KB20) and methanol blend (M5) fuelled transportation diesel engines. *Renewable Energy*, 98, pp.283-291.
- [2] Arrègle, J., López, J.J., Guardiola, C. and Monin, C., 2010. On board NOx prediction in diesel engines: a physical approach. In *Automotive model predictive control* (pp. 25-36). Springer, London.
- [3] Moos, R., 2005. A brief overview on automotive exhaust gas sensors based on electroceramics. *International Journal of Applied Ceramic Technology*, 2(5), pp.401-413.
- [4] Prasad, R.K. and Agarwal, A.K., 2018. Experimental evaluation of laser ignited hydrogen enriched compressed natural gas fueled supercharged engine. *Fuel*, 289, p.119788.
- [5] Egnell, R., 1998. Combustion diagnostics by means of multizone heat release analysis and NO calculation. *SAE transactions*, pp.691-710.
- [6] Timoney, D.J., Desantes, J.M., Hernández, L. and Lyons, C.M., 2005. The development of a semi-empirical model for rapid NO x concentration evaluation using measured in-cylinder pressure in diesel engines. *Proceedings of the Institution of Mechanical Engineers, Part D: Journal of Automobile Engineering*, 219(5), pp.621-631.
- [7] Cipolat, D., 2007. Analysis of energy release and NOx emissions of a CI engine fuelled on diesel and DME. *Applied Thermal Engineering*, 27(11-12), pp.2095-2103.
- [8] Hernández, J.J., Pérez-Collado, J. and Sanz-Argent, J., 2008. Role of the Chemical Kinetics on Modeling NO x Emissions in Diesel Engines. *Energy & fuels*, 22(1), pp.262-272.
- [9] Prasad, R.K., Mustafi, N. and Agarwal, A.K., 2018. Effect of spark timing on laser ignition and spark ignition modes in a hydrogen enriched compressed natural gas fuelled engine. *Fuel*, 276, p.118071.
- [10] Heywood JB. *Internal combustion engine fundamentals*. New York: McGraw-Hill, 1988.
- [11] Foster, D. E, "An Overview of Zero- Dimensional Thermodynamic Models for IC Engine Data Analysis", SAE 852070, 1985.
- [12] Johansson, B., Wilhelmsson, C., Tunestål, P., Johansson, R., & Widd, A. 2009. A Physical Two-Zone NOx Model Intended for Embedded Implementation. In *SAE World Congress*, 2009. SAE.

